IEEE Access
Multidisciplinary | Rapid Review | Open Access Journal

SPECIAL SECTION ON NON-ORTHOGONAL MULTIPLE ACCESS FOR 5G SYSTEMS

Received June 9, 2017, accepted July 2, 2017, date of publication July 17, 2017, date of current version September 27, 2017.

*Digital Object Identifier 10.1109/ACCESS.2017.2727518*

# When NOMA Meets Sparse Signal Processing: Asymptotic Performance Analysis and Optimal Sequence Design

**TING QI[1], (Student Member, IEEE), WEI FENG[2], (Member, IEEE), YUNFEI CHEN[3], (Senior Member, IEEE), AND YOUZHENG WANG[1], (Member, IEEE)**

[1]Tsinghua Space Center, Tsinghua University, Beijing 100084, China
[2]Tsinghua National Laboratory for Information Science and Technology, Department of Electronic Engineering, Tsinghua University, Beijing 100084, China
[3]School of Engineering, University of Warwick, Coventry CV4 7AL, U.K.

Corresponding author: Youzheng Wang (yzhwang@mail.tsinghua.edu.cn)

This work was supported in part by the Natural Science Foundation under Grant 61231011 and Grant 61321061, and in part by the National Basic Research Program of China under Grant 2013CB329001.

**ABSTRACT** Due to limited radio resources, non-orthogonal multiple access (NOMA) is a promising technology to enable massive connectivity in future 5G and beyond wireless networks. However, it suffers from the multiple access interference, which usually requires a high detection complexity to mitigate. In this paper, we consider NOMA with sparse multiple-access sequences, so as to leverage the message passing algorithm (MPA) for low-complexity and high-reliability multiuser detection. The optimal sparsity of spreading sequences is analyzed by minimizing the average bit error rate in the asymptotic large-system limit. Based on the analysis, the optimal sparse sequences that optimize the performance of MPA detector are designed in a systematically hierarchical way. The sparse structure is constructed given the target girth. Then, the values of nonzero entries are determined to maximize the minimum distance. The detection performance of the designed sparse sequences is presented for both additive white Gaussian noise and Rayleigh fading channels. Simulation results show the superiority of the proposed design in comparison with existing schemes.

**INDEX TERMS** Detection performance optimization, message passing algorithm (MPA), non-orthogonal multiple access (NOMA), sparse multiple-access sequences.

## I. INTRODUCTION

Non-orthogonal multiple access (NOMA) [1], [2] has been widely recognized as a promising technology to address the challenge of massive connectivity in future 5G wireless networks [3]. In NOMA, the system works in an overload way, i.e., $K$ users share $N$ orthogonal resources, e.g., time slots or orthogonal subcarriers, for $K > N$. Therefore, in NOMA systems, the multiple access interference (MAI) is usually severe, which should be carefully alleviated by using complicated multiuser detection (MUD).

### A. PRIOR WORKS

The way that $K$ users share $N$ resources can be described using a multiple-access matrix, denoted by $\boldsymbol{S}$, each column of which represents the spreading sequence of each user. Many schemes have been proposed to implement NOMA with relatively low implementation complexity. One widely researched scheme is to superpose the signals of two users and transmit them on one resource [4], and the corresponding matrix is simply $\boldsymbol{S} = \begin{bmatrix} 1 & 1 \end{bmatrix}$. Large gap between the channel gains of pairing users is expected so that successive interference cancellation MUD can be applied [5]. This scheme can achieve the sum capacity of the channel and can be extended to more than two users, and the system load, defined as $K/N$, takes integer values.

To achieve more diverse load, the matrix $\boldsymbol{S}$ has to be elaborately designed. Many researchers proposed to construct sparsely structured matrix so as to take advantage of sparse signal processing, i.e., the message passing algorithm (MPA) to largely reduce the practical complexity of MUD. The concept of sparse (also named low-density) spreading structure was introduced in [6], wherein the iterative soft-in-soft-out MUD based on MPA was studied and the advantage of this scheme was presented by simulation. This structure has further been applied to the orthogonal frequency division multiplexing system over the multipath fading channel and

achieved significant performance improvement [7]. Recently, sparse code multiple access that jointly designs symbol mapping and sparse sequences was proposed in [8]. The sparse matrices discussed in these works are generated randomly or found by trial-and-error.

When NOMA meets sparse signal processing, the key point lies in the multiple-access sequences. It is important to construct the optimal sparse sequences to achieve the best performance. The optimal sequences that can achieve both the sum capacity and the maximum sparsity were investigated in [9]. However, constructing the sparse matrix that optimizes the performance of the relevant MPA detector is more challenging, since there are no closed-form expressions for the relationship between the detection performance of MPA and the sparse sequences. Despite of the difficulty, the average performance can be evaluated by the asymptotic large-system limit analysis [10]–[13]. By establishing a probability density model for the entries of sparse spreading sequences, a method based on statistical mechanics was proposed to analyze the optimal detection performance [11] as well as the spectral efficiency of the scheme [10]. By letting the sparsity go to infinity at a smaller rate, the authors in [12] and [13] studied the performance of MPA and concluded that MPA detection for the sparsely spread system is asymptotically optimal. Besides the asymptotic large-system limit analysis, for finite-size multiuser systems, an iterative procedure utilizing the extrinsic information transfer chart was proposed in [14] to design the degree distribution for the low-density signature structure. Based on the sparse structure of low-density parity-check codes, the signature (value of non-zero entries) design was investigated in [15] and [16].

### B. CONTRIBUTION

The above mentioned works do not provide a systematic design of the optimal sparse sequences that optimizes the performance of MPA detector, especially with the constraints on the transmission efficiency and the detection complexity. It is critical for the practical application of NOMA to deal with the MAI with low-complexity and high-reliability. This motivates our work. The main contributions of the paper can be summarized as follows:

- We propose a systematic scheme to construct the sparse sequences in a hierarchical way with the aim of optimizing the performance of MPA. With this scheme, we are able to implement NOMA using sparse signal processing, i.e., MPA for low-complexity and high-reliability multiuser detection.
- We analyze the average BER of MPA in the asymptotic large-system limit by deriving the density evolution formula for the MPA detector, and formulate an optimization problem minimizing the average BER with the constraints on the system load and detection complexity. To solve the nonlinear integer programming problem, we propose an efficient algorithm to find the optimal sparsity.
- Based on the optimal sparsity using the large-system limit analysis, the optimal sparse sequences are designed in a hierarchical way. First, given the target girth, the sparse structure is constructed by leveraging the progressive edge growth method. Then, in regard to the choice of the values of nonzero entries, the minimum distance between two transmitted signals is maximized to further optimize the performance of MPA.
- The error performance of the designed sparse sequences is investigated for both AWGN and Rayleigh fading channels. The influence of constraints on the detection is illustrated, and the superiority of the proposed scheme is demonstrated in comparison with other schemes.

### C. ORGANIZATION

The rest of the paper is organized as follows. Section II presents the general system model of NOMA with sparse sequences, the factor graph representation and the MPA for multiuser detection. Section III performs the asymptotic large-system analysis of MPA and optimizes the sparsity by minimizing the average BER. The optimal sparse sequences are designed in a hierarchical way in Section IV. Section V evaluates the detection performance of the designed sparse sequences, and Section VI concludes the paper.

## II. SYSTEM MODEL

### A. NOMA WITH SPARSE SEQUENCES

Consider a NOMA system where $K$ users share $N$ orthogonal resources and $K > N$. The system load is defined as $\beta = \frac{K}{N}$, which measures the user capacity, the ability of accommodating users in the system and the efficiency of the system. Assume that each user is equipped with one antenna and consider the uplink channel where the users simultaneously transmit to the base station.

Let $x_k$ denote the transmitted symbol of user $k$ with a normalized average power of 1, i.e., $\mathbb{E}[x_k^2] = 1, \ \forall k = 1, \cdots, K$. Assume that the symbols $\{x_k\}$ take values from the constellation alphabet $\mathcal{X}$ with equal probability. In this paper, we consider binary phase-shift keying (BPSK) modulation, thus $\mathcal{X} = \{+1, -1\}$. Each user spreads its symbol onto the $N$ resources using a sequence. Let the spreading sequence of user $k$ be $\boldsymbol{s}_k = \frac{1}{\sqrt{\Lambda_k}}[s_{1k}, \ldots, s_{Nk}]^{\mathrm{T}}$ where $\frac{1}{\sqrt{\Lambda_k}}$ is the normalization factor such that $\|\boldsymbol{s}_k\|^2 = 1$. The symbol $x_k$ is modulated with the spreading sequence $\boldsymbol{s}_k$ with positive amplitude $A_k$. Assume that all symbols are transmitted with the same amplitude $A$. Let $\boldsymbol{x} = [x_1, x_2, \ldots, x_K]^{\mathrm{T}}$ be the transmitted vector and $\boldsymbol{S} = [\boldsymbol{s}_1, \ldots, \boldsymbol{s}_K]$ denote the multiple-access matrix, which represents the way users share the resources. The channel of user $k$ on the $N$ resources is denoted by the $N \times 1$ vector $\boldsymbol{h}_k$. The received signal, which is the superposed version of the transmitted signals from all users, can be written in discrete-form as

$$\begin{aligned} \boldsymbol{y} &= \sum_{k=1}^{K} A\boldsymbol{h}_k \odot \boldsymbol{s}_k x_k + \boldsymbol{w} \\ &= A\boldsymbol{H} \odot \boldsymbol{S}\boldsymbol{x} + \boldsymbol{w}, \end{aligned} \tag{1}$$

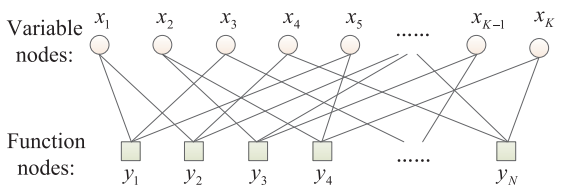


**FIGURE 1.** The factor graph representation of sparse sequences with $d_v = 2$ and $d_f = 3$.

where $\boldsymbol{y} = [y_1, y_2, \ldots, y_N]^{\mathrm{T}}$ is the received signal vector collected from the $N$ resources, and $\boldsymbol{w} \sim \mathcal{CN}(\boldsymbol{0}, \boldsymbol{I})$ denotes the white Gaussian noise vector, $\odot$ represents the entrywise product and $\boldsymbol{H} = [\boldsymbol{h}_1, \ldots, \boldsymbol{h}_K]$ is the channel matrix. The channel considered here is either AWGN channel, where $h_{nk} = 1, \forall n, k$, or Rayleigh fading channel, where $h_{nk}$ follows i.i.d $\mathcal{CN}(0, 1)$. The signal-to-noise ratio (SNR) of each user is equal to $20 \log_{10} A$ dB.

To reduce the detection complexity, the matrix $\boldsymbol{S}$ is designed to be sparse so as to leverage the low-complexity MPA detection to achieve near optimal performance. Specifically, each symbol is spread over a relatively small number of the $N$ resources and each resource is used by a relatively small number of the $K$ users. We define an $N \times K$ binary indicator matrix, denoted by $\boldsymbol{G} = \{g_{nk}\}_{N \times K}$, where '1's indicate the nonzero entries in $\boldsymbol{S}$, i.e., for $\forall n, k$, if $g_{nk} = 0$, set $s_{nk} = 0$; if $g_{nk} = 1$, set $s_{nk} \neq 0$. With $\boldsymbol{S}$ being sparse, the signal model (1) can be represented by the factor graph, where the transmitted symbol $x_k$, denoted by variable node, and the received symbol $y_n$, denoted by function node, are connected by edge $e_{k,n}$ if $g_{nk} = 1$, and the gain corresponding to the edge is $\frac{s_{nk} h_{nk}}{\sqrt{\Lambda_k}} A$.

The variable and function node sparsity are defined as the number of edges connected with them, respectively and also equal to the number of nonzero entries in columns and rows of the matrix $\boldsymbol{S}$. The matrix $\boldsymbol{S}$ is regular if the variable nodes and the function nodes are of identical sparsity respectively, otherwise it is irregular. Regular matrices potentially outperform irregular ones in terms of spectral efficiency and bit error probability [11]. Therefore, in this paper, we focus on regular structures. Let $d_v$ and $d_f$ denote the variable and function node sparsity respectively, and we have $d_v = \sum_{n=1}^{N} g_{nk}, \forall k$ and $d_f = \sum_{k=1}^{K} g_{nk}, \forall n$. Fig. 1 shows the factor graph of sparse sequences with $d_v = 2$ and $d_f = 3$. For regular structures, the following relationship must be satisfied:

$$\beta = \frac{d_f}{d_v}. \tag{2}$$

### B. MPA DETECTION

MPA is an iterative detection performed over the factor graph. In each iteration, messages that measure the a *posterior* probability of the variable node are sent to the connected function nodes; each function node then computes messages to send back to the variable nodes based on the observed signal and the previously received messages. For detailed description, we refer the readers to [6]. Let $v_{k\to n}^{(t)}$ and $u_{n\to k}^{(t)}$ be the messages sent along edge $e_{k,n}$ between variable node $x_k$ and function node $y_n$ in the $t$-th iteration. The messages are represented in the form of log-likelihood ratio (LLR) for BPSK. The update equations are given by (3) and (4) (on bottom the next page).

$$v_{k\to n}^{(t)} = \sum_{j \in \zeta_k \backslash n} u_{j\to k}^{(t-1)}, \tag{3}$$

where $\zeta_k$ ($\zeta_n$) is the index subset of function (variable) nodes connected to $x_k$ ($y_n$), called its neighborhood; $\zeta_k \setminus n$ denote the neighborhood of $x_k$ excluding $y_n$.

The initial condition of the iteration is $v_{k\to n}^{(0)} = 0$. After the messages have converged or the maximum number of iterations $T$ has been met, all the messages coming to variable node $x_k$ are summed to compute the final LLR $v_{k\to n} = \sum_{j \in \zeta_k} u_{j\to k}^{(T)}$, which can be used to make a final decision for symbol $x_k$ or be sent to the following decoding module.

## III. ASYMPTOTIC LARGE-SYSTEM ANALYSIS

As there is no closed-form expression for the relationship between the detection performance of MPA and the sparse sequences, it is intractable to optimize the sparse sequences directly. To overcome this difficulty, we firstly investigate the performance of MPA in the asymptotic large-system limit, by letting $K, N \to \infty$ with their ratio $\beta$ fixed.

In the large-system limit, the average bit error rate (BER) will be evaluated for the limiting variable and function node sparsity of the matrix, based on which an optimization problem that minimizes the average BER is formulated with constraints on the system load and detection complexity. We perform the large-system limit analysis by adopting the density evolution (DE) framework. It was first introduced to calculate the threshold of the sum-product decoding [17] and was used to search for the capacity-approaching low-density parity check codes (LDPC) [18]. DE is an effective tool for analyzing the dynamic behavior of belief-propagation-like algorithms. We will first derive the DE formula for the MPA detector and analyze the impact of sparsity on the performance. We then formulate an optimization problem to minimize the average BER with the constraints of system load demand and detection complexity. An efficient algorithm is proposed to obtain the optimal variable and function node sparsity.

### A. ANALYSIS OF MPA BY DENSITY EVOLUTION

Assume that the indicator matrix $\boldsymbol{G}$ is uniformly and randomly picked from the indicator matrix ensemble for the given sparsity distribution. Nonzero entry $s_{nk}$ is drawn i.i.d from the distribution $p_s$ with zero mean and unit variance. Average performance will be evaluated by DE.

Large-system limit renders the random sparse graphs to be locally tree-like, which ensures that the incoming messages are independent. DE treats the sent messages as independent random variables, and tracks the probability density

function (PDF) of the messages. Without loss of generality, assume that all inputs are $+1$ and that the messages follow Gaussian distribution. This approximation has good performance as elaborated in [17], and we will show later that it is valid in this case. Moreover, the MPA detector fulfills the symmetry condition [13], which leads to $\sigma^2 = 2m$ for a Gaussian distribution with mean $m$ and variance $\sigma^2$. Thus, tracking the mean of the message is enough, which dramatically reduces the computational complexity of DE.

Let $v$ and $u$ be the message from a variable node and a function node, respectively. The DE formula for the MPA detector is given as follows.

*Theorem 1:* Denote $m_u$ and $m_v$ as the mean of $u$ and $v$, respectively. Then, $m_u$ and $m_v$ are calculated by (5) and (6) in the $t$-th iteration, respectively, written as

$$m_u^{(t)} = \frac{2A^2}{d_v} \int_{-\infty}^{\infty} \frac{1}{\alpha \frac{4e^v}{(e^v+1)^2} + 1} \cdot \frac{1}{4\pi m_v^{(t)}} e^{-\frac{(v-m_v^{(t)})^2}{4m_v^{(t)}}} \mathrm{d}v, \quad (5)$$

$$m_v^{(t)} = (d_v - 1) m_u^{(t-1)}, \quad (6)$$

where $\alpha = \frac{d_f - 1}{d_v} A^2$. The initial condition is

$$m_u^{(0)} = \frac{2A^2}{d_v(\alpha + 1)}. \quad (7)$$

*Proof:* See the appendix. ■

After the maximum number of iterations $T$ has been met or the messages have converged, the final message $v$ follows a Gaussian distribution $\mathcal{N}(m_v^*, 2m_v^*)$ with $m_v^* = d_v m_u^{(T)}$. The equivalent average SNR is $m_v^*/2$ and the BER is given by

$$\mathrm{BER} = Q\left(\sqrt{m_v^*}\right), \quad (8)$$

where $Q(x)$ is the $Q$-function of standard normal distribution.

We will use the derived DE formula (5) and (6) to evaluate the performance of MPA in the large-system limit and provide some insights on the influence of sparsity and system load.

Fig. 2 shows the asymptotic average BER achieved by the MPA detector for various sparsity settings $(d_v, d_f)$ and fixed load $\beta = 1.5$. The single user bound, which is the BER of orthogonal multiple access system (OMA) system, is also plotted for comparison. It reveals that the performance of MPA approaches the single user bound as SNR increases. It is observed that, for fixed system load, the performance improves with increasing sparsity in the medium and high SNR regime, and the improvement reduces as the sparsity increases further. This feature is further examined in Fig. 3, which plots the variation of the BER vs. sparsity for different

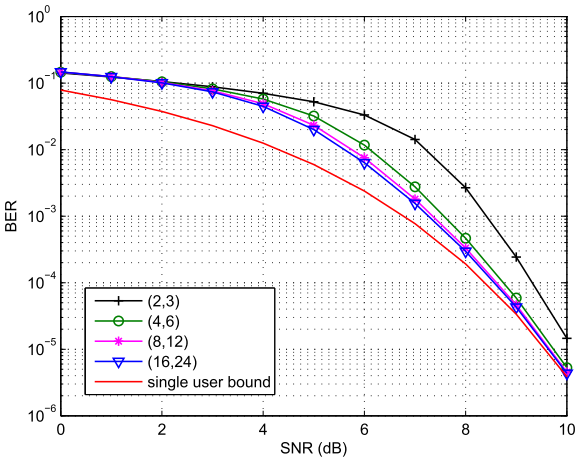


**FIGURE 2.** The asymptotic average BER of MPA in large-system limit for various sparsity settings $(d_v, d_f)$ and the fixed load $\beta = 1.5$.

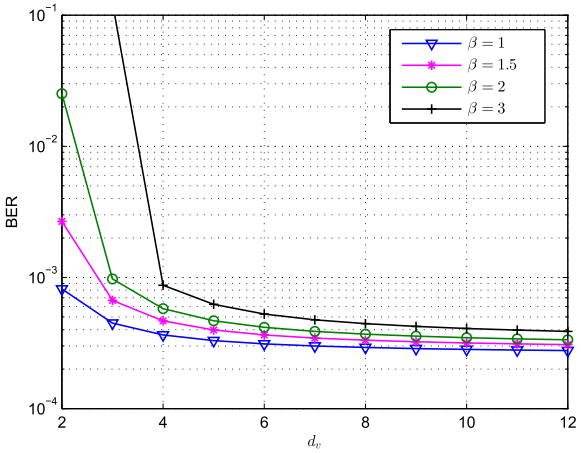


**FIGURE 3.** The variation of the asymptotic average BER vs. sparsity for different fixed system loads and SNR = 8 dB.

fixed system loads. The performance is improved dramatically when $d_v$ increases from 2 to 6 and remains approximately the same when $d_v$ is beyond 6.

Fig. 4 presents the variation of BER vs. the system load given SNR = 8 dB. The BER performance becomes worse as the system load increases, as expected. Moreover, there is a threshold of system load for each variable sparsity, beyond which the performance deteriorates rapidly.

### B. OPTIMIZATION OF SPARSITY

Denote $P_e$ as the average BER performance of MPA detector in the asymptotic large-system limit. According to the

$$u_{n\to k}^{(t)} = \log \frac{\sum_{\substack{i\in\zeta_n\backslash k \\ x_k=+1}} \exp\left(-\frac{1}{2}(y_n - \sum_{i\in\zeta_n} \frac{s_{ni}h_{ni}}{\sqrt{\Lambda_i}} A x_i)^2 + \sum_{i\in\zeta_n\backslash k} \frac{x_i}{2} v_{i\to n}^{(t)}\right)}{\sum_{\substack{i\in\zeta_n\backslash k \\ x_k=-1}} \exp\left(-\frac{1}{2}(y_n - \sum_{i\in\zeta_n} \frac{s_{ni}h_{ni}}{\sqrt{\Lambda_i}} A x_i)^2 + \sum_{i\in\zeta_n\backslash k} \frac{x_i}{2} v_{i\to n}^{(t)}\right)}, \quad (4)$$

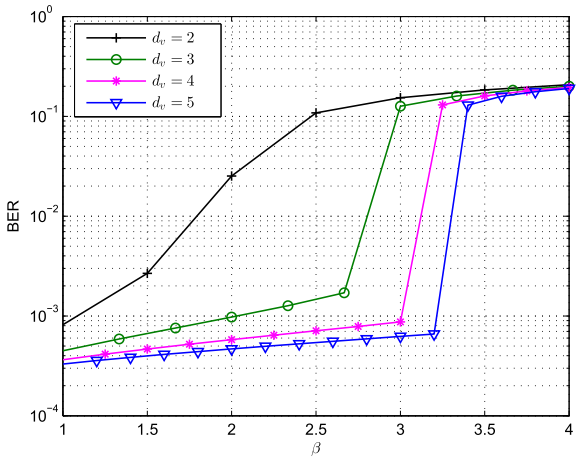


**FIGURE 4.** The variation of the asymptotic average BER vs. system load under SNR = 8 dB.

previous analysis, $P_e$ is a function of $d_f$ and $d_v$ when SNR is fixed. We formulate an optimization problem that minimizes the average BER with the constraints on the system load and the detection complexity. The optimization problem is given by

$$\min_{d_v,\, d_f} \quad P_e \tag{9a}$$

$$\text{s.t.} \quad \beta \geq \beta_0, \tag{9b}$$

$$d_f \leq \overline{d}_f, \tag{9c}$$

$$d_v, d_f \in \mathbb{N}^+ \geq 2, \tag{9d}$$

where $\beta_0$ is the required minimum system load, and inequation (9c) gives the detection complexity constraint, because the complexity of MPA is $\mathcal{O}(|\mathcal{X}|^{d_f})$ [15]. Constraint (9d) means $d_v$ and $d_f$ can only take positive integer values larger than 2. With these objective function and constraints, we have formulated a nonlinear integer programming problem.

This problem is hard to solve because no analytic expression can be derived for $P_e\left(d_v, d_f\right)$, as MPA is a nonlinear iterative detection method. By leveraging the previous analysis of MPA and investigating the characteristics of the problem, we will propose an efficient algorithm to search for the optimal solution.

*Theorem 2:* If we extend the feasible region to the real domain, i.e., remove the integer constraint (9d), the optimal solution to (9a) is obtained when constraints (9b) and (9c) are satisfied with equality simultaneously.

*Proof:* Suppose there exists an optimal sparsity pair $(d_v', d_f')$, for which one of the following three cases is valid: 1) $\beta' = \beta_0$, $d_f' < \overline{d}_f$; 2) $\beta' > \beta_0$, $d_f' = \overline{d}_f$; 3) $\beta' > \beta_0$, $d_f' < \overline{d}_f$, where $\beta' = \frac{d_f'}{d_v'}$.

For case 1), keep $\beta'$ fixed and increase $(d_f', d_v')$ to $(d_f^{(1)}, d_v^{(1)})$ so that $d_f^{(1)} = \overline{d}_f$. This will improve the detection performance, i.e., $P_e(d_v^{(1)}, d_f^{(1)}) < P_e(d_v', d_f')$, so that $(d_v', d_f')$ is not optimal. For case 2), decrease $\beta'$ by increasing $d_v'$ so that the detection performance is improved. For case 3) we can verify that $(d_v', d_f')$ is not optimal in a similar manner. Thus the proposition is true. ■

**TABLE 1.** Proposed algorithm for design of optimal sparsity.

**Input:** Given SNR, the system load demand $\beta_0$, complexity constraint parameter $\overline{d}_f$
**Output:** Optimal sparsity $(d_v^*, d_f^*)$.

Initialize $d_f^* = \overline{d}_f$, $d_v^* = \lfloor d_v' \rfloor$ with $\overline{d}_f / d_v' = \beta_0$, $i = 1$, $d_v^{(1)} = d_v^*$, $d_f^{(1)} = d_f^*$;
**while** $d_v^{(i)} > 1$
  **if** the current load $d_f^{(i)} / d_v^{(i)} \geq \beta_0$
    **if** $P_e(d_f^{(i)}, d_v^{(i)}) \leq P_e(d_f^*, d_v^*)$
      Update the current optimal sparsity $(d_v^*, d_f^*) = (d_v^{(i)}, d_f^{(i)})$;
    **end**
    **if** $d_f^{(i)} > d_v^{(i)} + 1$
      Update $(d_v^{(i+1)}, d_f^{(i+1)}) = (d_v^{(i)} + 1, d_f^{(i)})$;
    **else**
      Update $(d_v^{(i+1)}, d_f^{(i+1)}) = (d_v^{(i)}, d_f^{(i)} - 1)$;
    **end**
  **else**
    Update $(d_v^{(i+1)}, d_f^{(i+1)}) = (d_v^{(i)} - 1, d_f^{(i)} - 1)$;
  **end**
  $i = i + 1$;
**end**

When the integer constraint is added, the optimal sparsity pair may not be the point that satisfies constraints (9b) and (9c) with equality any more, but it will be close to the optimal value. Based on this observation, an algorithm is proposed in TABLE 1, where $\lfloor z \rfloor$ means getting the largest integer smaller than or equal to $z$. The algorithm starts from the integer point nearest to the boundary of the feasible region and searches along the descent direction of objective function. The total number of points possible to be searched is evaluated to be $(d_f^{(1)} - 2)(d_v^{(1)})$. Therefore, the complexity of the algorithm is $\mathcal{O}\left((\overline{d}_f - 2)\lfloor \frac{\overline{d}_f}{\beta_0} \rfloor\right)$. Since the searching space is limited, the algorithm will converge after a few loops. In each loop, the algorithm can search all the points superior to the current one in the feasible region. Thus the solution of the algorithm is optimal.

We will give the optimization results for various configurations of constraint parameters.

*Result 1:* Given SNR = 8dB and the system load demand $\beta_0 = 1.5$, the optimal sparsity under various $\overline{d}_f$ settings is presented in TABLE 2.

*Result 2:* Given SNR = 8dB and the complexity constraint parameter $\overline{d}_f = 6$, the optimal sparsity under various load $\beta_0$ is presented in TABLE 3.

## IV. SPARSE SEQUENCES DESIGN

Based on the large-system limit analysis, in the following, the optimal sparse sequences that optimize the performance of MPA detector is designed in a systematically hierarchical way, as illustrated in Fig. 5. First, the dimensions of the matrix are determined and the sparse structure is constructed

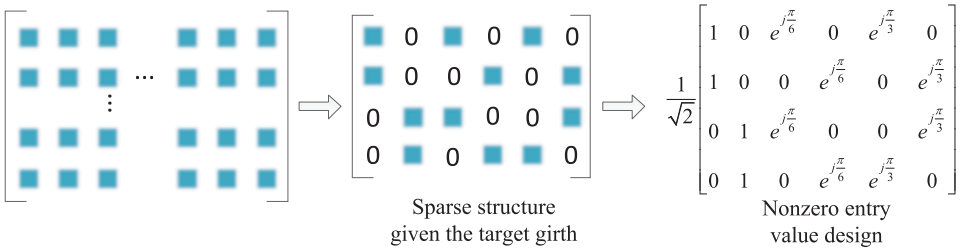


**FIGURE 5.** The schematic diagram of the proposed hierarchical scheme for the sparse sequences design.

**TABLE 2.** The optimal sparsity under various $\bar{d}_f$, SNR=8 dB, $\beta_0 = 1.5$.

| $\bar{d}_f$ | 3 | 4 | 5 | 6 | 7 | 8 | 9 |
|---|---|---|---|---|---|---|---|
| $d_v^*$ | 2 | 2 | 3 | 4 | 4 | 5 | 6 |
| $d_f^*$ | 3 | 3 | 5 | 6 | 6 | 8 | 9 |
| $P_e^*$ | 2.7e-3 | 2.7e-3 | 7.6e-4 | 4.7e-4 | 4.7e-4 | 4.1e-4 | 3.6e-4 |

**TABLE 3.** The optimal sparsity under various load, SNR=8 dB, $\bar{d}_f = 6$.

| $\beta_0$ | 1 | 1.2 | 1.5 | 1.6 | 2 | 2.5 | 3 |
|---|---|---|---|---|---|---|---|
| $d_v^*$ | 6 | 5 | 4 | 3 | 3 | 2 | 2 |
| $d_f^*$ | 6 | 6 | 6 | 5 | 6 | 5 | 6 |
| $P_e^*$ | 3.1e-4 | 3.6e-4 | 4.7e-4 | 7.6e-4 | 9.7e-4 | 0.11 | 0.15 |

given the target girth. This step gives the indicator matrix. Then, the values of nonzero entries are designed with the aim of maximizing the minimum Euclidean distance of the transmitted vector, to optimize the detection performance.

### A. SPARSE STRUCTURE DESIGN

Given the variable and function node sparsity, the next step is to design the sparse structure that gives the position of nonzero entries in the matrix. This is performed under the condition of limited dimension, which may lead to cycles in the factor graph. The MPA over cycle-free factor graphs provide optimal detection, but cycles especially small cycles deteriorate the performance of MPA. Hence it is necessary to mitigate the influence of the cycles. The girth of a factor graph is defined as the length of the smallest cycle in the graph, and the smaller the girth, the worse the performance will be.

To guarantee the performance, a tolerable girth is set for this procedure and the goal is to construct the factor graph with girth meeting the requirement from an ensemble of factor graphs given the sparsity.

The problem of constructing sparse factor graphs was widely researched in LDPC [19]. Typical LDPC construction methods is introduced as follows. Gallager's construction is based on a banded structure in check matrix with random submatrices. There is no guarantee that small cycles are not present. Progressive edge growth (PEG) is a graph based method, where edges are added to the factor graph progressively in an edge-by-edge manner, so as to maximize the local girth at the current variable node. Thus, PEG method avoids the occurrence of small cycles [20], and it is adopted in this paper to generate the indicator matrix, given the sparsity.

The following proposition gives the range of the number of resources so as to satisfy the girth requirements with the given sparsity.

*Theorem 3:* Consider a regular indicator matrix with variable sparsity $d_v$ and function sparsity $d_f$. Given the desired girth $g$, the number of rows in the matrix, denoted by $N$, is in the interval $[N_l, N_u)$ where

$$N_l = \frac{[(d_f-1)(d_v-1)]^{\frac{g-2}{4}}-1}{1-\frac{d_v}{d_f(d_v-1)}}+1,$$
$$N_u = \frac{[(d_f-1)(d_v-1)]^{\frac{g}{2}}-1}{d_f-\frac{d_f}{d_v}-1} \tag{10}$$

*Proof:* The girth $g$ is lower bounded and upper bounded by $g \geq 2(\lfloor t \rfloor + 2)$ and $g \leq 4\lfloor t \rfloor + 2$, respectively [20] where

$$t = \frac{\log(Nd_f - \frac{Nd_f}{d_v} - N + 1)}{\log[(d_v-1)(d_f-1)]} - 1. \tag{11}$$

Therefore we have the bound for $t$ given by

$$\frac{g-2}{4} \leq t < \frac{g}{2} - 1. \tag{12}$$

Substituting (11) into (12) and solving (12), we can obtain the lower and upper bound given in (10). ■

There are actually multiple factor graphs satisfying the girth requirement. We will select the one with minimum dimension in order to make the system more flexible. The algorithm to generate the optimal sparse structure is listed in TABLE 4.

The following example gives the constructed indicator matrices, denoted by $\boldsymbol{G}_{(d_v,d_f),g}$, given the target girth $g$ and sparsity $(d_v, d_f)$.

*Result 3:* Given $(d_v, d_f) = (2, 3)$, if we set the target girth $g = 6$, the indicator matrix is

$$\boldsymbol{G}_{(2,3),6} = \begin{bmatrix} 1 & 0 & 1 & 0 & 1 & 0 \\ 1 & 0 & 0 & 1 & 0 & 1 \\ 0 & 1 & 1 & 0 & 0 & 1 \\ 0 & 1 & 0 & 1 & 1 & 0 \end{bmatrix}, \tag{13}$$

**TABLE 4. Algorithm for the construction of optimal indicator matrix.**

| |
|---|
| **Input:** Given sparsity $d_v$ and $d_f$, the minimum girth $g$, |
| **Output:** Optimal indicator matrix $\boldsymbol{G}$. |
| Calculate $N_l$ and $N_u$ by (10); |
| $N = \lceil \frac{N_l}{d_v} \rceil d_v, K = \lceil \frac{N_l}{d_v} \rceil d_f$; |
| **loop** |
| Construct the sparse indicator matrix $\boldsymbol{G}$ by the PEG algorithm with input $N, K, d_v, d_f$; |
| $N = N + d_v, K = K + d_f$; |
| **until** the girth of $\boldsymbol{G}$ is not smaller than $g$ |

if we set the target girth $g = 8$, the indicator matrix is then

$$\boldsymbol{G}_{(2,3),8} = \begin{bmatrix} 1&1&1&0&0&0&0&0&0&0&0&0 \\ 0&0&0&1&1&1&0&0&0&0&0&0 \\ 0&0&0&0&0&0&1&1&1&0&0&0 \\ 0&0&0&0&0&0&0&0&0&1&1&1 \\ 0&1&0&0&0&1&0&1&0&0&0&0 \\ 0&0&1&0&1&0&0&0&0&1&0&0 \\ 1&0&0&0&0&0&0&0&1&0&0&1 \\ 0&0&0&1&0&0&1&0&0&0&1&0 \end{bmatrix}. \tag{14}$$

### B. NONZERO ENTRY VALUE DESIGN

This section addresses the problem of choosing the values of nonzero entries in the matrix $\boldsymbol{S}$ for the best detection performance. The distance spectrum, related to the matrix and the constellation alphabet, determines the performance of optimal detection. The distance between two arbitrary transmitted vectors $\boldsymbol{x}_1, \boldsymbol{x}_2 \in \mathcal{X}$ is defined by $D = \|A\boldsymbol{S}(\boldsymbol{x}_1 - \boldsymbol{x}_2)\|$. Let $\Delta\mathcal{X} = \{0, \pm 2\}$ and $\Delta\mathcal{X}^K$ be the set of length $K$ vectors with entries taken values from $\Delta\mathcal{X}$. The minimum distance is thus given by

$$D_m = \min_{\Delta\boldsymbol{x}\in\Delta\mathcal{X}^K, \Delta\boldsymbol{x}\neq\boldsymbol{0}} D(\boldsymbol{S}, \Delta\boldsymbol{x}).$$
$$D(\boldsymbol{S}, \Delta\boldsymbol{x}) = \sqrt{\sum_{n=1}^{N} \left| \sum_{k=1}^{K} \frac{1}{\sqrt{\Lambda_k}} A s_{nk} \Delta x_k \right|^2} \tag{15}$$

Since constant-modulus value is in favor of implementation, we assume the nonzero entries $s_{nk} = e^{j\theta}, \theta \in [0, 2\pi)$ for $h_{nk} = 1$ and denote $\mathcal{S}$ as the matrix set with such unit-modulus value. Particularly, the BER is approximately proportional to $e^{-D_m}$ at high SNR. Therefore, given the indicator matrix, we design the optimal matrix with the maximum minimum distance.

However, finding the optimal matrix is generally an intractable problem with high complexity. The following proposition provides a method of reducing the size of searching space.

*Proposition 1:* (*[16],Theorem 3*) Let $\boldsymbol{G}$ be the indicator matrix with cycles in the corresponding factor graph and denote $E$ as the edge subset that after delating the edges inside, the graph becomes a tree. The optimal matrix with the maximum minimum distance is in the subset $\{\boldsymbol{S} | s_{nk} = e^{j\theta_k}, \theta_1 = 0, \theta_2, \cdots, \theta_K \in [0, \frac{\pi}{2})$ for $e_{n,k} \in \bar{E}$ and $s_{nk} = e^{j\theta_{nk}}, \theta_{nk} \in [0, 2\pi)$ for $e_{n,k} \in E\}$.

Nevertheless, it is still complicated to search for the optimal matrix when $\boldsymbol{G}$ is of relatively large dimension or sparsity. To simplify the problem, an efficient way is to limit the non-zero entries of each row of $\boldsymbol{S}$ to take values from the same finite constellation, represented by $\{a_i\}$, and the size of the constellation equals to the function sparsity $d_f$. Specifically, non-zero entries of each row take distinct values from $\{a_i\}$, $i = 0, 1, \cdots, d_f - 1$. Furthermore, let $\{a_i\}$ satisfy the row-wise unique decodability requirement, that is for two distinct transmitted vector $\boldsymbol{x}_1, \boldsymbol{x}_2$ and $\boldsymbol{x}_1 \neq \boldsymbol{x}_2$, $\boldsymbol{S}\boldsymbol{x}_1 \neq \boldsymbol{S}\boldsymbol{x}_2$ element-wisely, which guarantees that $\boldsymbol{S}$ is uniquely decodable. A empirically good design based on extensive simulation is [15]

$$a_i = \exp\left(j\frac{2\pi}{C}i\right), \ i = 0, 1, \cdots, d_f - 1, \tag{16}$$

where $C = \frac{4d_f}{\gcd(2, d_f)}$ is chosen to get good distance spectrum.

Let $\boldsymbol{S}_{(d_v,d_f)(N,K)}$ represent the designed $N \times K$ multiple-access matrix with sparsity $(d_v, d_f)$. In the following, a simple example is given to demonstrate the design procedure.

*Example 1:* Setting $\beta_0 = 1.5, \bar{d}_f = 3$ and given SNR=8dB, the optimal sparsity is $(2, 3)$ according to TABLE 1. Then let the target girth $g = 6$ and the constructed optimal indicator matrix is shown by (13). The value constellation is $a_i = \exp(j\frac{\pi}{6}i), \ i = 0, 1, 2$ according to (16). Thus the constructed matrix is

$$\boldsymbol{S}_{(2,3)(4,6)} = \frac{1}{\sqrt{2}} \begin{bmatrix} 1&0&e^{j\frac{\pi}{6}}&0&e^{j\frac{\pi}{3}}&0 \\ 1&0&0&e^{j\frac{\pi}{6}}&0&e^{j\frac{\pi}{3}} \\ 0&1&e^{j\frac{\pi}{6}}&0&0&e^{j\frac{\pi}{3}} \\ 0&1&0&e^{j\frac{\pi}{6}}&e^{j\frac{\pi}{3}}&0 \end{bmatrix}. \tag{17}$$

Other matrices for various parameter settings can be constructed in a similar way.

## V. NUMERICAL RESULTS AND DISCUSSION

In this section, we simulate the BER performance of the designed sparse sequences under different conditions. Firstly, we will depict the performance of MPA for AWGN channel and investigate the influence of constraints.

Fig. 6 presents the performance of three sparse matrices designed with various complexity parameter $\bar{d}_f$, identical system load $\beta_0 = 1.5$ and target girth $g = 6$. The single user bound is provided as a benchmark, as the optimal performance for OMA. It can be seen that the detection complexity can be traded for better performance approaching the single user bound in high SNR regime. Our NOMA scheme using the designed matrices $\boldsymbol{S}_{(3,5)(48,80)}$ and $\boldsymbol{S}_{(4,6)(228,342)}$ can accommodate 50% more users than OMA scheme with a

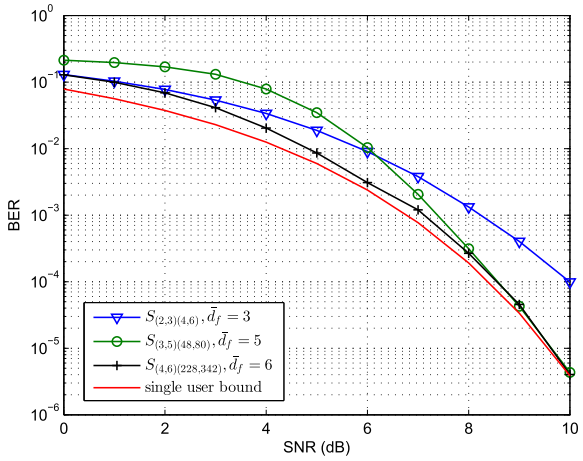


**FIGURE 6.** The average BER under matrices with various $\bar{d}_f$, the same $\beta_0 = 1.5$ and $g = 6$.

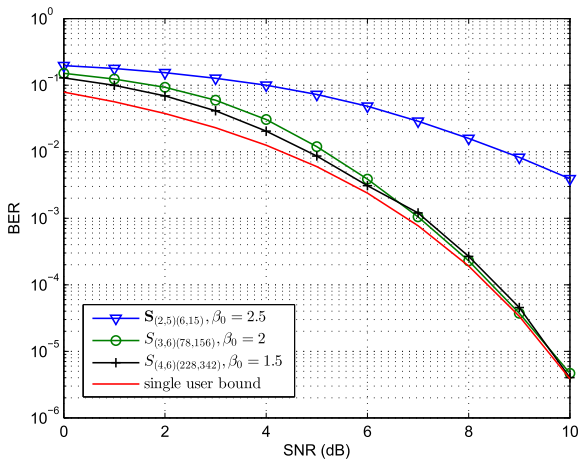


**FIGURE 7.** The average BER under matrices with various $\beta_0$, the same $\bar{d}_f = 6$ and $g = 6$.

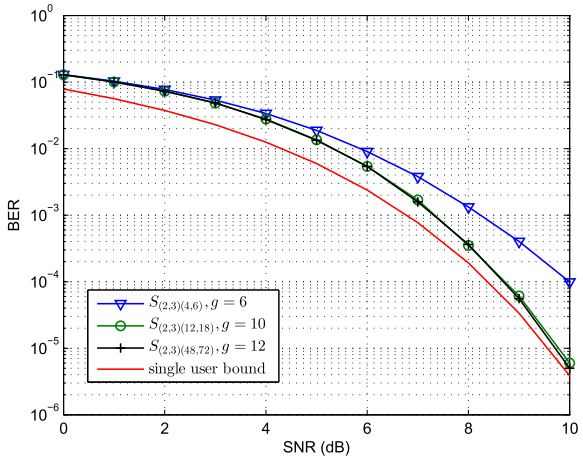


**FIGURE 8.** The average BER under matrices with various girth, the same $\beta_0 = 1.5$ and $\bar{d}_f = 3$.

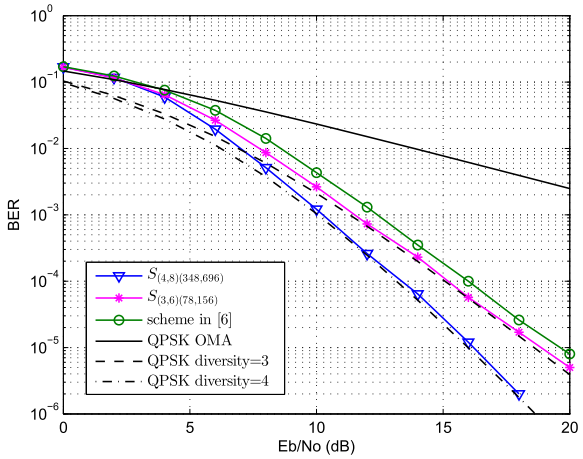


**FIGURE 9.** The average BER in Rayleigh fading channel when the rates of various schemes are identical.

performance loss of only about 0.07dB at BER $= 10^{-5}$ over the single user bound.

The performance of sparse matrices for various system loads is shown in Fig. 7 for the same complexity parameter and target girth. The increasing load incurs performance loss and especially, increasing the load from 2 to 2.5 aggravates the loss, which is also demonstrated in Fig. 4. Despite the high load, $\boldsymbol{S}_{(3,6)(78,156)}$ achieves an excellent BER performance, almost as good as $\boldsymbol{S}_{(4,6)(228,342)}$ at high SNR.

Fig. 8 illustrates the performance of sparse matrices for various girths when $\beta_0 = 1.5$ and $\bar{d}_f = 3$. Note that not all girth setting can obtain corresponding regular sparse matrix, for example for sparsity $(2, 3)$, $g = 8$ regular sparse matrix cannot be found. Given the sparsity, girth influences the dimension of the matrix and the optimality of MPA detection. It shows that the performance of $\boldsymbol{S}_{(2,3)(48,72)}$ and $\boldsymbol{S}_{(2,3)(12,18)}$ have very small gap but are better than $\boldsymbol{S}_{(2,3)(4,6)}$. This implies that large girth improves the performance, but the impact becomes weaker as girth increases.

Assuming perfect channel state information at the receiver, we simulate the performance of the proposed scheme over Rayleigh fading channel. Fig. 9 gives the average BER performance of $\boldsymbol{S}_{(4,8)(348,696)}$ and $\boldsymbol{S}_{(3,6)(78,156)}$ with the system load $\beta = 2$. The performance of the NOMA scheme in [7] with also 200% overload and OMA with QPSK modulation are provided for comparison. It reveals that the proposed NOMA scheme outperforms the other two while achieving the same spectral efficiency. It can be observed that the proposed NOMA scheme is able to obtain the diversity gain in fading channel through spreading the signal over several resources. The diversity gain the NOMA scheme can obtain is approximately the same as the designed variable sparsity. The theoretical BER of OMA-QPSK with diversity gain being 3 and 4 are also plotted to verify the observation.

## VI. CONCLUSION

In this paper, we consider the NOMA with sparse multiple-access sequences, so as to leverage the message passing algorithm (MPA) to largely reduce the practical complexity

of MUD. Particularly, the optimal sparse sequences that optimize the performance of MPA detector have been investigated. To make the problem tractable, the optimal sparse sequences are designed in a systematically hierarchical way. The optimal sparsity of sequences is analyzed by minimizing the average BER in the asymptotic large-system limit. On this basis, the sparse structure is constructed given the target girth and then the values of nonzero entries are chosen with the aim of maximizing the minimum distance. Simulation results have shown the detection performance of the designed sparse sequences in both AWGN and Rayleigh fading channel. It shows that by careful choice of parameters, the performance of the sparse NOMA schemes can approach the single user bound at high SNR while supporting system overload. The superiority of the proposed scheme in Rayleigh fading channel due to the ability of obtaining diversity gain is revealed.

## Appendix

### Proof of Theorem 1

According to (3), $v$ is equal to the sum of the incoming messages from other connected function nodes, denoted by $u_j, j = 1, \cdots, d_v - 1$, i.e.,

$$v = \sum_{j=1}^{d_v-1} u_j. \tag{18}$$

Since $u_j$'s are i.i.d. and have the same mean, the mean of $v$ at the $t$-th iteration is updated as

$$m_v^{(t)} = (d_v - 1)m_u^{(t-1)}. \tag{19}$$

To calculate $m_u$, Gaussian approximation for interference is exploited. Specifically, the signal received at resource $n$ can be written as

$$y_n = \frac{s_{nk}h_{nk}}{\sqrt{\Lambda_k}}Ax_k + z_{nk}, \tag{20}$$

where $z_{nk} = \sum_{i\in\zeta_n\backslash k} \frac{s_{ni}h_{ni}}{\sqrt{\Lambda_i}}Ax_i + w_n$ contains interference and Gaussian noise. When $d_v$ is large enough, the central limit theorem works; then $z_{nk}$ approximately follows a Gaussian distribution $\mathcal{N}(\mu_z, \sigma_z^2)$ with

$$\mu_z = \sum_{i\in\zeta_n\backslash k} \frac{s_{ni}h_{ni}}{\sqrt{\Lambda_i}}A\mathbb{E}(x_i), \tag{21}$$

$$\sigma_z^2 = \sum_{i\in\zeta_n\backslash k} \frac{|s_{ni}|^2|h_{ni}|^2}{\Lambda_i}A^2\mathrm{Var}(x_i) + 1, \tag{22}$$

where $\mathbb{E}(x_i)$ and $\mathrm{Var}(x_i)$ denote mean and variance of $x_i$ respectively, written as

$$\mathbb{E}(x_i) = \frac{e^{v_{i\to n}} - 1}{e^{v_{i\to n}} + 1}, \tag{23}$$

$$\mathrm{Var}(x_i) = \frac{4e^{v_{i\to n}}}{(e^{v_{i\to n}} + 1)^2}. \tag{24}$$

Therefore, the message $u_{n\to k}^{(t)}$ reduces to

$$u_{n\to k}^{(t)} = \frac{2}{\sigma_z^{2(t)}}\frac{s_{nk}^*h_{nk}^*}{\sqrt{\Lambda_k}}A(y_n - \mu_z^{(t)}). \tag{25}$$

Given $s_{nk}$, $h_{nk}$ and $y_n$, taking the mean of (25) over $v$ with distribution $\mathcal{N}(m_v, 2m_v)$, we obtain (we omit $(t)$ for brevity)

$$m_u(\boldsymbol{S}, \boldsymbol{H}, y_n) = \frac{2s_{nk}^*h_{nk}^*}{\sqrt{\Lambda_k}}A\left[\mathbb{E}_v(\frac{1}{\sigma_z^2})y_n - \mathbb{E}_v(\frac{\mu_z}{\sigma_z^2})\right]. \tag{26}$$

For all $+1$ input, we have $y_n \sim \mathcal{N}(\sum_{i\in\zeta_n}\frac{s_{ni}h_{ni}}{\sqrt{\Lambda_i}}A, 1)$. Note that the nonzero entries of $\boldsymbol{S}$ are i.i.d variables with zero mean and unit variance, and $h_{nk}$ is either equal to 1 or follows Gaussian distribution with zero mean and unit variance. Taking the expectation over the randomness of $\boldsymbol{S}$, $\boldsymbol{H}$ and $y_n$, the first term and the second term in the right of (26) respectively equal to

$$\mathbb{E}\left[\frac{2s_{nk}^*h_{nk}^*}{\sqrt{\Lambda_k}}Ay_n\mathbb{E}_v(\frac{1}{\sigma_z^2})\right] = \frac{2A^2}{d_v}\mathbb{E}_v\left(\frac{1}{\alpha\mathrm{Var}(x_i) + 1}\right), \tag{27}$$

$$\mathbb{E}\left[\frac{2s_{nk}^*h_{nk}^*}{\sqrt{\Lambda_k}}A\mathbb{E}_v(\frac{\mu_z}{\sigma_z^2})\right] = 0. \tag{28}$$

Substituting (27) and (28) into (26), we can obtain (5). To begin with, because of no message from the observed signal, let $\mathbb{E}(x_i) = 0, \mathrm{Var}(x_i) = 1$ to obtain the initial condition.

## REFERENCES

[1] Z. Ding *et al.*, "Application of non-orthogonal multiple access in LTE and 5G networks," *IEEE Commun. Mag.*, vol. 55, no. 2, pp. 185–191, Feb. 2017.
[2] L. Dai, B. Wang, Y. Yuan, S. Han, C.-L. I., and Z. Wang, "Non-orthogonal multiple access for 5G: Solutions, challenges, opportunities, and future research trends," *IEEE Commun. Mag.*, vol. 53, no. 9, pp. 74–81, Sep. 2015.
[3] W. Feng, Y. Wang, D. Lin, N. Ge, J. Lu, and S. Li, "When mmWave communications meet network densification: A scalable interference coordination perspective," *IEEE J. Sel. Areas Commun.*, vol. 35, no. 7, pp. 1459–1471, Jul. 2017.
[4] Y. Saito, A. Benjebbour, Y. Kishiyama, and T. Nakamura, "System-level performance of downlink non-orthogonal multiple access (NOMA) under various environments," in *Proc. IEEE 81st Veh. Technol. Conf. (VTC Spring)*, May 2015, pp. 1–5.
[5] Z. Ding, P. Fan, and H. V. Poor, "Impact of user pairing on 5G nonorthogonal multiple-access downlink transmissions," *IEEE Trans. Veh. Technol.*, vol. 65, no. 8, pp. 6010–6023, Aug. 2015.
[6] R. Hoshyar, F. P. Wathan, and R. Tafazolli, "Novel low-density signature for synchronous CDMA systems over AWGN channel," *IEEE Trans. Signal Process.*, vol. 56, no. 4, pp. 1616–1626, Apr. 2008.
[7] R. Hoshyar, R. Razavi, and M. Al-Imari, "LDS-OFDM an efficient multiple access technique," in *Proc. IEEE 71st Veh. Technol. Conf.*, May 2010, pp. 1–5.
[8] H. Nikopour and H. Baligh, "Sparse code multiple access," in *Proc. IEEE 24th Annu. Int. Symp. Pers., Indoor, Mobile Radio Commun. (PIMRC)*, Sep. 2013, pp. 332–336.
[9] T. Qi, W. Feng, and Y. Wang, "Optimal sequences for non-orthogonal multiple access: A sparsity maximization perspective," *IEEE Commun. Lett.*, vol. 21, no. 3, pp. 636–639, Mar. 2017.
[10] M. Yoshida and T. Tanaka, "Analysis of sparsely-spread CDMA via statistical mechanics," in *Proc. IEEE Int. Symp. Inf. Theory*, Jul. 2006, pp. 2378–2382.
[11] J. Raymond and D. Saad, "Sparsely spread CDMA—A statistical mechanics-based analysis," *J. Phys. A, Math. Theor.*, vol. 40, pp. 12315–12333, Sep. 2007.
[12] D. Guo and C.-C. Wang, "Multiuser detection of sparsely spread CDMA," *IEEE J. Sel. Areas Commun.*, vol. 26, no. 3, pp. 421–431, Apr. 2008.

[13] A. Montanari and D. Tse, "Analysis of belief propagation for non-linear problems: The example of CDMA (or: How to prove Tanaka's formula)," in *Proc. IEEE Inf. Theory Workshop*, Mar. 2006, pp. 160–164.
[14] T. Huang, J. Yuan, X. Cheng, and W. Lei, "Design of degrees of distribution of LDS-OFDM," in *Proc. IEEE 9th Int. Conf. Signal Process. Commun. Syst. (ICSPCS)*, Dec. 2015, pp. 1–6.
[15] J. van de Beek and B. M. Popovic, "Multiple access with low-density signatures," in *Proc. IEEE Global Telecommun. Conf.*, Nov./Dec. 2009, pp. 1–6.
[16] G. Song, X. Wang, and J. Cheng. (Apr. 2016). "Signature design of sparsely spread CDMA based on superposed constellation distance analysis." [Online]. Available: https://arxiv.org/abs/1604.04362
[17] S.-Y. Chung, T. J. Richardson, and R. L. Urbanke, "Analysis of sum-product decoding of low-density parity-check codes using a Gaussian approximation," *IEEE Trans. Inf. Theory*, vol. 47, no. 2, pp. 657–670, Feb. 2001.
[18] T. J. Richardson, M. A. Shokrollahi, and R. L. Urbanke, "Design of capacity-approaching irregular low-density parity-check codes," *IEEE Trans. Inf. Theory*, vol. 47, no. 2, pp. 619–637, Feb. 2001.
[19] S. J. Johnson. *Introducing Low-Density Parity-Check Codes*. [Online]. Available: http://sigpromu.org/sarah/SJohnsonLDPCintro.pdf
[20] X.-Y. Hu, E. Eleftheriou, and D.-M. Arnold, "Progressive edge-growth tanner graphs," in *Proc. IEEE Global Telecommun. Conf.*, Nov. 2001, pp. 995–1001.

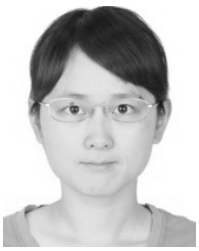

**TING QI** received the B.S. degree (Hons.) from the School of Telecommunication and Information Engineering, Nanjing University of Posts and Telecommunications, Nanjing, China, in 2013. She is currently pursuing the Ph.D. degree with the School of Aerospace Engineering, Tsinghua University, Beijing, China. Her research interests include non-orthogonal multiple access technology, and 5G and coordinated satellite-terrestrial networks.

**WEI FENG** (S'06–M'10) received the B.S. and Ph.D. degrees (Hons.) from the Department of Electronic Engineering, Tsinghua University, Beijing, China, in 2005 and 2010, respectively. From 2010 to 2011, he served as a Project Director of the National Science and Technology Major Project Management Office, Tsinghua University. From 2011 to 2014, he was a Post-Doctoral Research Fellow with the Department of Electronic Engineering, Tsinghua University, where he has been an Assistant Professor until 2014, and then an Associate Professor since 2016. He has authored over 70 journal and conference papers. He also holds over 10 granted patents. His research interests include maritime broadband communication networks, large-scale distributed antenna systems, and coordinated satellite-terrestrial networks. He has received the Outstanding Ph.D. Graduate of Tsinghua University Award in 2010, the IEEE WCSP Best Paper Award in 2013, the First Prize of Science and Technology Award of China Institute of Communications in 2015, the IEEE WCSP Best Paper Award in 2015, and the second Prize of National Technological Invention Award of China in 2016. He currently serves as the Assistant to the Editor-in-Chief of the *China Communications*.

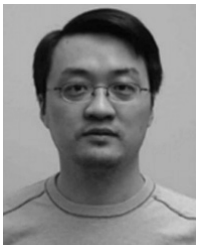

**YUNFEI CHEN** (S'02–M'06–SM'10) received the B.E. and M.E. degrees in electronic engineering from Shanghai Jiao Tong University, China, in 1998 and 2001, respectively, and the Ph.D. degree from the University of Alberta, Canada, in 2006. He is currently with the College of Computer and Information, Hohai University, Nanjing, China. He is also with the School of Engineering, Warwick University, Coventry, U.K. His research interests include energy harvesting, wireless relaying, and general performance analysis and design of wireless systems.

**YOUZHENG WANG** received the B.S., M.S., and Ph.D. degrees in electronic engineering from Tsinghua University, Beijing, China, in 1992, 1997, and 2009, respectively. Since 1997, he has been with the Department of Electronic Engineering, Tsinghua University, where he has been on the Research Staff and then promoted to an Associate Professor in 2004. He is currently an Associate Professor with the Department of Aeronautics and Astronautics Engineering, Tsinghua University. His research interests are resource allocation, cooperative communication, satellite communication, and maritime communication.